International Journal of Heat and Mass Transfer 55 (2012) 3412–3422

Contents lists available at SciVerse ScienceDirect

International Journal of Heat and Mass Transfer

journal homepage: www.elsevier.com/locate/ijhmt

Effects of temperature dependent properties in electromagnetic heating

Mohammad Robiul Hossan, Prashanta Dutta *

School of Mechanical and Materials Engineering, Washington State University, Pullman, WA 99164-2920, United States

ARTICLE INFO

Article history:
Received 22 July 2011
Received in revised form 17 February 2012
Accepted 17 February 2012

Keywords:
Electromagnetic heating
Microwave
Radio frequency heating
Integral transform technique

ABSTRACT

Electromagnetic heating such as microwave processing and radio frequency heating becomes very popular because of its non-contact, pollution free and fast distribution of thermal energy within the object of interest. In electromagnetic heating, the temperature distribution within a sample greatly depends on the dielectric properties which are functions of electromagnetic frequency, temperature and the composition of the object. There are many experimental and numerical investigations on electromagnetic heating because of its widespread use in food and other industries, but only few researchers have looked at this problem from analytic point of view specifically for the temperature dependent properties. In this paper, we developed an analytic expression for temperature distribution in a three dimensional rectangular object under electromagnetic heating and presented a method to incorporate temperature dependent properties of the object in determining the temperature distribution at different times. A simplified Maxwell's equation is solved for plane wave to obtain electric field distribution in the body, and the electromagnetic power absorption is computed from the electric field distribution which was then used as a source term in the energy equation. Next an unsteady, three dimensional, non-homogenous energy equation is solved by integral transform technique to obtain temperature distribution. Finally, this closed form analytical solution is used to study the effects of electromagnetic frequency, dielectric properties, and heat transfer coefficient on temperature distribution in a rectangular salmon fillet. It is found that incident frequency, sample thickness and processing time have significant influence on the heating pattern. For radio frequency heating, the temperature dependent dielectric properties influence the temperature distribution significantly, but the effect of temperature dependent dielectric properties is less dominant for the microwave frequency used in the household microwave oven. Our results also show that microwave heating provides heterogeneous temperature distribution with alternate hot and cold spots. On the other hand, the radio frequency heating allows almost uniform temperature distribution within the body, which makes it a better choice for quick and convenient heating process especially for commercial and industrial heating.

1. Introduction

In recent days electromagnetic heating is getting popularity as an alternative heating technique in many industries such as wood, textile, biotechnology, materials, and food processing. The efficacy of the electromagnetic heating primarily depends on the ability of a material to absorb electromagnetic energy and convert it to thermal energy [1]. This ability of a material is reflected by dielectric properties: dielectric constant and dielectric loss. The dielectric constant is the capacity of a material to store electric energy, whereas the dielectric loss is the measure of the electrical energy dissipation into heat. The electromagnetic heating offers fast, non-contact, and pollution free heating with material selective heat generation.

Material selective heat generations can be used in fabrication of polymer based micro/nanofluidic device [2,3] and sintering process. Generally in this type of fabrication process, the electromagnetic heating is exploited for bonding purpose by introducing a very thin layer (100 nm–1 micron thick) of highly dielectric material between two layers. As the electromagnetic waves pass through the highly dielectric material it gets melted, and hence two layers can be bonded irreversibly at moderate pressure. In addition to the manufacturing process, the electromagnetic heating can be applied in various biotechnology applications such as polymerase chain reaction (PCR), temperature induced cell lysis, organic and inorganic chemical synthesis, drug delivery, etc. [2,4–6]. Electromagnetic heating is also very convenient for processing of low thermal conductive material such as food items as heat starts flowing from the interior of material body to the outer surface. As a matter of fact, the single largest user of electromagnetic heating is the food industry where it is used for thawing, warming, cooking, tempering, blanching, sterilization, etc. [7].

* Corresponding author. Tel.: +1 509 335 7989; fax: +1 509 335 4662.
E-mail address: prashanta@wsu.edu (P. Dutta).

0017-9310/$ - see front matter © 2012 Elsevier Ltd. All rights reserved.
doi:10.1016/j.ijheatmasstransfer.2012.02.072

Nomenclature

a	length of the object (m)
$\vec{B}$	magnetic induction (Wb/m^2)
b	thickness of the object (m)
c	velocity of light (m/s)
c_p	specific heat capacity (J/kg K)
$\vec{D}$	electric displacement (C/m^2)
$\vec{E}$	electric field (V/m)
E_x	electric field in x-direction (V/m)
f	frequency (Hz)
$\vec{H}$	magnetic field (A/m)
$\vec{H}^*$	complex conjugate of $\vec{H}$ (A/m)
H_y	magnetic field in y-direction (A/m)
h	heat transfer coefficient (W/m^2 K)
$\vec{J}$	current density (A/m^2)
K	kernel
k	thermal conductivity (W/m K)
$\vec{P}$	Poynting power flux vector (W/m^2)
$\dot{Q}$	power generation (W/m^3)
R_{01}	reflection coefficient
T	Temperature (°C)
t	time (s)
T_{01}	transmission coefficient
w	width of the object (m)
X	decomposed temperature in x-direction (°C)
x	location along x coordinate (m)
y	location along y coordinate (m)
z	location along z coordinate (m)

Greek symbols

α	thermal diffusivity (m^2/s)
β	attenuation factor (rad/m)
χ	propagation constant (m^{-1})
δ	reflection phase angle (rad)
ε	permittivity (F/m)
ε_0	free-space permittivity (F/m)
γ	ratio of heat transfer coefficient and thermal conductivity (m)
η	eigenvalues in the z-direction
κ'	relative dielectric constant
κ''	relative dielectric loss
λ	eigenvalues in the x-direction
μ	permeability (H/m)
μ_0	free-space permeability (H/m)
θ	modified temperature (°C)
ρ	density (kg/m^3)
ρ_v	charge density (C/m^3)
σ	phase factor (rad/m)
σ'	electrical conductivity (S/m)
ζ	impedance (ohm)
ω	angular frequency (rad/s)
ξ	eigenvalues in the y-direction

Subscripts

i	initial
n	eigenvalue index
p	eigenvalue index
q	eigenvalue index
∞	surrounding
0	free space
1	within food/object

The electromagnetic heating can be divided into two major categories primarily based on the frequency of the incident wave: radio frequency heating (<300 MHz) and microwave heating (300–3000 MHz). Microwave heating is very popular in food industries as well as in home and office to warm up foodstuffs quickly. However, the heterogeneous energy absorption in microwave processing leads to uneven temperature distribution in the object. The non-uniform temperature distribution not only affects the quality of food but also raises serious concerns for food safety. Uneven heating of foodstuff may leave bacteria or pathogens alive in cold spots and may cause various food borne diseases. Goksoy et al. [8] found that microwave cooking produces islands of cold spots in poultry meat that facilitates optimum thermal environment for microorganism growth. On the other hand, radio frequency heating generally provides uniform heating with low energy consumption [9].

In electromagnetic heating process, a number of factors are responsible for thermal energy flow within the object. Among them material composition, dielectric characteristics, sample size and shape, and incident wave frequency are most important. In an experimental study, Jeong et al. [10] reported that the presence of salt in meat increase the processing time and non-uniformity of temperature distribution in microwave heating. The heterogeneity in temperature distribution is also observed in microwave thawing as the dielectric properties vary significantly in frozen and defrosted zones [1]. In recent years, the effects of size, shape, moisture content, and dielectric properties have been studied both experimentally and numerically for radio frequency [9,11–13] and microwave [7,8,10–19] heating.

Although there exist extensive experimental and numerical studies on electromagnetic heating, only a handful of studies used analytic techniques to analyze the fundamentals of electromagnetic heating. A close-form analytic expression for temperature can be obtained for some simplified problems and these types of solutions can reveal the correlation among the characteristics of electromagnetic wave, dielectric and thermo-physical properties of material subjected to microwave or radio frequency heating. Fleischman [20] provided a one dimensional temperature distribution for microwave heating. Lately, Hossan et al. [21] presented 3D analytical solution for the temperature distribution within a cylindrical shaped object for microwave heating. All previous analytic works assumed constant dielectric properties for a particular working frequency. However, experimental works [22–23] indicate changes in dielectric properties within the object as the temperature increases with time. This variation is very significant at the lower end of the electromagnetic frequency [22]. The temperature dependent dielectric properties alters the absorption capability of electromagnetic energy and penetration depth, and hence the nature of transient temperature distribution. Therefore, to predict the temperature accurately, one has to consider temperature dependent property change in the energy equation, especially for the electromagnetic source term. In this paper, we presented an analytical expression for temperature distribution within a three dimensional rectangular block subjected to electromagnetic heating and proposed an algorithm to evaluate temperature distribution in an object with temperature dependent dielectric properties.

The rest of the paper is organized as follows. First, the theory and governing equations for electromagnetic heating are provided.

Then, an analysis to find the electromagnetic power generation from electromagnetic wave is presented. Next, the temperature distribution within an object is obtained from the energy equation using integral transform technique for a short period of processing time, and then a method is presented to implement temperature dependent material properties for subsequent time steps. This is followed by a discussion on electromagnetic heating of salmon fillet for various heat transfer coefficients and incident frequencies. Finally, we present our conclusions on this analytic work.

2. Theory

Electromagnetic heating is generally very effective for a dielectric medium where heat generation takes place due to the dielectric polarization [24]. When an electric field is applied across a dielectric medium, the positive and negative charges are aligned toward cathode and anode respectively forming dipoles. These dipoles rotate as they try to align themselves with the alternating electric field of the electromagnetic waves. Therefore, to study the electromagnetic heating one has to understand the electromagnetic field within the system as well as its effects on energy equation.

2.1. Governing equations

The electromagnetic field distribution within a material is governed by Maxwell's equation as [25]:

$$\vec{\nabla}\times\vec{E}=-\frac{\partial\vec{B}}{\partial t} \tag{1a}$$

$$\vec{\nabla}\times\vec{H}=\vec{J}+\frac{\partial\vec{D}}{\partial t} \tag{1b}$$

$$\vec{\nabla}\cdot\vec{D}=\rho_v \tag{1c}$$

$$\vec{\nabla}\cdot\vec{B}=0 \tag{1d}$$

where $\vec{E}$ is the electric field, $\vec{B}$ is the magnetic induction, $\vec{H}$ is the magnetic field, $\vec{J}$ is the current density, $\vec{D}$ is the electric displacement, and ρ_v is the electric charge density. The time averaged power flux associated with the electromagnetic wave can be obtained as Poynting vector [25]:

$$\vec{P}=\frac{1}{2}\left(\vec{E}\times\vec{H}^{*}\right) \tag{2a}$$

where $\vec{H}^{*}$ is the complex conjugate of magnetic field. The volumetric heat generation can be obtained as

$$\dot{Q}=Re(-\vec{\nabla}\cdot\vec{P}) \tag{2b}$$

For electromagnetic heating, the temperature distribution within the system is governed by the energy equation as [25]:

$$\rho C_p\frac{dT}{dt}=\vec{\nabla}\cdot\left(k\vec{\nabla}T\right)+\dot{Q} \tag{3}$$

The left hand side term represents the rate of thermal energy change in the system, while the first term in the right hand side accounts for the thermal diffusion.

2.2. Assumptions

In this study, we considered a 3D rectangular shaped object (Fig. 1) which is subjected to electromagnetic heating. For simplicity, we assume that electromagnetic waves are transverse (TEM) or uniform plane waves. Although a uniform plane wave cannot be formed in a real system, the electric field distribution obtained from this simplified TEM model can approximate the actual electric field in the rectangular system [25]. In TEM, both electric and magnetic fields are normal to the direction of propagation (Fig. 1). The other assumptions used to simplify the problem are:

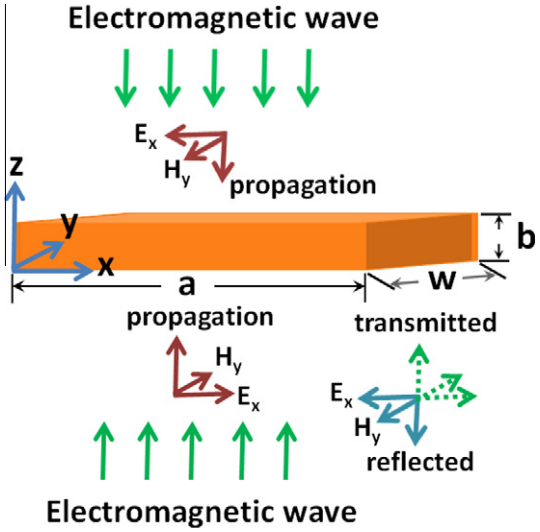

Fig. 1. Schematic of a three dimensional rectangular object heated by electromagnetic wave. In a uniform plane wave, the magnetic field is always perpendicular to the electric field. The length, width, and height of the object are *a*, *w*, and *b*, respectively.

(i) The object of interest obeys linear material constitutive laws.
(ii) Electroneutrality condition is satisfied within the system.
(iii) The magnetic permeability $\mu(\omega)$ can be approximated by its value in free space
(iv) The effect of moisture is not modeled explicitly, but it is taken into consideration through temperature dependent dielectric properties of the material. This is reasonable for electromagnetic heating as the dielectric properties are very strong function of material composition.
(v) Material properties, such as thermal conductivity and specific heat are temperature independent.

3. Analysis

3.1. Electromagnetic power

Maxwell's equations can be simplified by using the assumptions mentioned above and by applying following material constitutive relations [25]

$$\vec{J}=\sigma'\vec{E} \tag{4a}$$

$$\vec{D}=\varepsilon\vec{E} \tag{4b}$$

$$\vec{B}=\mu\vec{H} \tag{4c}$$

where σ' is the electrical conductivity, ε is the permittivity, and μ is the magnetic permeability. If electromagnetic incident rays are propagating in the *z*-direction, the only non-zero component of electric field is $E=E_x$. Therefore, for system shown in Fig. 1, the simplified equation for electric field can be written as [7]:

$$\frac{d^2E}{dz^2}+\chi^2E=0 \tag{5}$$

where χ is the propagation constant, and it can be given as $\chi^2=\omega^2\mu_0\varepsilon_0(\kappa'+i\kappa'')$. The propagation constant can also be expressed as $\chi=\sigma+i\beta$, where the phase factor and the attenuation factor can be given by Eqs. (6a) and (6b), respectively [7]

$$\sigma = \frac{2\pi f}{c}\sqrt{\frac{\kappa'\left(\sqrt{1+\tan^2\delta}+1\right)}{2}} \tag{6a}$$

$$\beta = \frac{2\pi f}{c}\sqrt{\frac{\kappa'\left(\sqrt{1+\tan^2\delta}-1\right)}{2}} \tag{6b}$$

For a uniform plane electromagnetic wave propagating in the z direction of a rectangular block (Fig. 1), the boundary conditions at the top and bottom surfaces are given by

$$E_0 = E_1 \tag{7a}$$

$$\frac{1}{\mu_0\omega}\frac{dE_0}{dz} = \frac{1}{\mu_1\omega}\frac{dE_1}{dz} \tag{7b}$$

where 0 and 1 indicate the free and object, respectively. The electric field distribution within the object of interest can be expressed as:

$$E = \frac{T_{01}E_0}{1+R_{01}e^{i\chi_1 b}}\left(e^{i\chi_1 z}+e^{i\chi_1(b-z)}\right) \tag{8}$$

where the transmission and the reflection coefficients are

$$T_{01} = \frac{2\zeta_1}{\zeta_1+\zeta_0} \tag{9a}$$

$$R_{01} = \frac{\zeta_1-\zeta_0}{\zeta_1+\zeta_0} \tag{9b}$$

and the intrinsic impedance [25] is

$$\zeta = \frac{\mu\omega}{\chi} \tag{9c}$$

On the other hand, if the electromagnetic waves come from the one (bottom) side of the block, then the electric field distribution is:

$$E = \frac{T_{01}E_0}{1-R_{01}^2e^{i2\chi_1 b}}\left(e^{i\chi_1 z}+R_{01}e^{i\chi_1(2b-z)}\right) \tag{10}$$

Once the electric field distribution is known, the magnetic field distribution can be evaluated eventually as they are related by

$$\frac{dE_x}{dz} = i\mu\omega H_y \tag{11}$$

Now applying Poynting power theorem, the power dissipated per unit volume can be calculated as [7]:

$$\dot{Q} = \frac{1}{2}\omega\varepsilon_0\kappa''|E|^2 \tag{12}$$

and the volumetric power generation within the sample can be obtained as:

$$\dot{Q} = \frac{1}{2}\omega\varepsilon_0\kappa''|E_0|^2|T_{01}|^2 \times \frac{e^{-2\beta z}+e^{-2\beta(b-z)}+2\cos(2\sigma z-\sigma b)e^{-\beta b}}{1+2|R_{01}|e^{-\beta b}\cos(\delta_{01}+\sigma b)+|R_{01}|^2e^{-2\beta b}} \tag{13a}$$

Similarly, for one (bottom) sided incidence of electromagnetic wave, the volumetric power generation within the food slab can be obtained as:

$$\dot{Q} = \frac{1}{2}\omega\varepsilon_0\kappa''|E_0|^2|T_{01}|^2 \times \frac{e^{-2\beta z}-2|R_{01}|e^{-2\beta b}\cos(\delta_{01}+2\sigma(b-z))+|R_{01}|^2e^{-2\beta(2b-z)}}{1-2|R_{01}|^2e^{-2\beta b}\cos(2\delta_{01}+2\sigma b)+|R_{01}|^4e^{-4\beta b}} \tag{13b}$$

It is important to note that the source terms presented in Eqs. (13a) and (13b) are a function of temperature (T) in addition to the location (z) in the direction of wave propagation. The temperature dependency comes from the dielectric properties such as dielectric loss and dielectric constant in the phase factor and the attenuation factor as well as from transmission and reflection coefficients.

3.2. Heat equation and temperature distribution

The energy equation for a three dimensional rectangular block (Fig. 1) subjected to electromagnetic heating can be simplified as

$$\frac{\partial^2T}{\partial x^2}+\frac{\partial^2T}{\partial y}+\frac{\partial^2T}{\partial z^2}+\frac{\dot{Q}(T,z)}{k} = \frac{1}{\alpha}\frac{\partial T}{\partial t} \quad \text{in} \quad 0\leqslant x<a;\ 0\leqslant y<w;\quad 0<z<b \tag{14}$$

where α is the thermal diffusivity, k is the thermal conductivity, and T is the temperature. The initial and boundary conditions for the system shown in Fig. 1 are:

$$T = T_i \quad \text{at} \quad t=0 \tag{15a}$$

$$k\frac{\partial T}{\partial x} = h(T-T_\infty) \quad \text{at} \quad x=0;\quad t>0 \tag{15b}$$

$$-k\frac{\partial T}{\partial x} = h(T-T_\infty) \quad \text{at} \quad x=a;\quad t>0 \tag{15c}$$

$$k\frac{\partial T}{\partial y} = h(T-T_\infty) \quad \text{at} \quad y=0;\quad t>0 \tag{15d}$$

$$-k\frac{\partial T}{\partial y} = h(T-T_\infty) \quad \text{at} \quad y=w;\quad t>0 \tag{15e}$$

$$k\frac{\partial T}{\partial z} = h(T-T_\infty) \quad \text{at} \quad z=0;\quad t>0 \tag{15f}$$

$$-k\frac{\partial T}{\partial z} = h(T-T_\infty) \quad \text{at} \quad z=b;\quad t>0 \tag{15g}$$

The governing equation presented in (14) is nonlinear due to the temperature dependent source term. Hence, finding a close-form analytic expression for this system is not trivial. However, one can consider the problem as linear if the temperature distribution is sought for a very short period of processing time within which the variation in dielectric properties is negligible due to small temperature change within the body. Here our approach is to solve the above second order, nonhomogenous partial differential equation using integral transform technique for a short, but finite period of time assuming temperature independent source term, and then use the solution as initial condition for the next time step. Hence our next step is to solve Eq. (14) for a short period of time ($t \to t+\tau$). For electromagnetic heating, the value of τ could be $\leqslant$1 s in which the generation term remains almost constant. Thus, for a short period (τ) of electromagnetic heating, the governing equation for $\theta = T - T_\infty$ with temperature independent source term becomes

$$\frac{\partial^2\theta}{\partial x^2}+\frac{\partial^2\theta}{\partial y^2}+\frac{\partial^2\theta}{\partial z^2}+\frac{\dot{Q}(z)}{k} = \frac{1}{\alpha}\frac{\partial\theta}{\partial t} \quad \text{in } 0\leqslant x<a;\ 0\leqslant y<w;\quad 0<z<b \tag{16}$$

The initial and boundary conditions for the above equation become

$$\theta = \theta_i \tag{17a}$$

$$-\frac{\partial\theta}{\partial x}+\gamma\theta = 0 \quad \text{at} \quad x=0 \tag{17b}$$

$$\frac{\partial\theta}{\partial x}+\gamma\theta = 0 \quad \text{at} \quad x=a \tag{17c}$$

$$-\frac{\partial\theta}{\partial y}+\gamma\theta = 0 \quad \text{at} \quad y=0 \tag{17d}$$

$$\frac{\partial\theta}{\partial y}+\gamma\theta = 0 \quad \text{at} \quad y=w \tag{17e}$$

$$-\frac{\partial\theta}{\partial z}+\gamma\theta = 0 \quad \text{at} \quad z=0 \tag{17f}$$

$$\frac{\partial\theta}{\partial z}+\gamma\theta = 0 \quad \text{at} \quad z=b \tag{17g}$$

where $\gamma = \frac{h}{k}$. The partial derivative with respect to x can be eliminated from energy Eq. (16) by introducing Fourier transform as [26]

$$\bar{\theta}(\lambda_n, y, z, t) = \int_0^a K(\lambda_n, x)\theta(x, y, z, t)dx \tag{18}$$

where the kernels $K(\lambda_n, x)$ are the characteristic functions of the following eigenvalue problem:

$$\frac{d^2X}{dx^2} + \lambda^2 X^2 = 0 \tag{19}$$

$$-\frac{dX}{dx} + \gamma X = 0 \quad \text{at} \quad x = 0 \tag{20a}$$

$$\frac{dX}{dx} + \gamma X = 0 \quad \text{at} \quad x = a \tag{20b}$$

where λ is the eigenvalue. For the above eigenvalue problem, the kernel can be found as $K(\lambda_n, x) = \frac{\sqrt{2}(\lambda_n \cos \lambda_n x + \gamma \sin \lambda_n x)}{\sqrt{a(\lambda_n^2+\gamma^2)+2\gamma}}$. The eigenvalues λ_n are the positive roots of

$$\tan(\lambda_n a) = \frac{\lambda_n(2\gamma)}{\lambda_n^2 - \gamma^2} \tag{21}$$

The transformation of energy Eq. (16) with respect to x, through the use of Eq. (18) yields

$$-\lambda_n^2\bar{\theta} + \frac{\partial^2\bar{\theta}}{\partial y^2} + \frac{\partial^2\bar{\theta}}{\partial z^2} + \frac{\bar{\dot{Q}}(z)}{k} = \frac{1}{\alpha}\frac{\partial\bar{\theta}}{\partial t} \tag{22}$$

where $\bar{\dot{Q}}(z) = \dot{Q}(z)\left[\sin(\lambda_n a) - \frac{\gamma}{\lambda_n}\cos(\lambda_m a) + \frac{\gamma}{\lambda_n}\right]$. Similarly the partial derivative with respect to y and z are removed by Fourier transform and the energy equation becomes an ordinary differential equation with respect to time (t) as

$$-\alpha\left(\lambda_n^2 + \xi_p^2 + \eta_q^2\right)\bar{\bar{\bar{\theta}}} + \Phi = \frac{d\bar{\bar{\bar{\theta}}}}{dt} \tag{23}$$

where

$$\Phi = \left[\sin(\lambda_n a) - \frac{\gamma}{\lambda_n}\cos(\lambda_n a) + \frac{\gamma}{\lambda_n}\right]\left[\sin(\xi_p w) - \frac{\gamma}{\xi_p}\cos(\xi_p w) + \frac{\gamma}{\xi_p}\right] \times \int_0^b Q(z)\left(\eta_q \cos\eta_q z + \gamma \sin\eta_q z\right)dz \tag{24}$$

Here the eigenvalues in the y and z directions can be found from $\tan(\xi_p w) = \frac{\xi_p(2\gamma)}{\xi_p^2 - \gamma^2}$ and $\tan(\eta_q b) = \frac{\eta_q(2\gamma)}{\eta_q^2 - \gamma^2}$, respectively. Now the ordinary differential equation (Eq. (23)) for transformed temperature ($\bar{\bar{\bar{\theta}}}$) can be solved as

$$\bar{\bar{\bar{\theta}}}\left(\lambda_n, \xi_p, \eta_q, t\right) = \frac{\Phi}{\alpha\left(\lambda_n^2 + \xi_p^2 + \eta_q^2\right)}\left(1 - e^{-\alpha\left(\lambda_n^2+\xi_p^2+\eta_q^2\right)\tau}\right) + \bar{\bar{\bar{\theta}}}_i e^{-\alpha\left(\lambda_n^2+\xi_p^2+\eta_q^2\right)\tau} \tag{25}$$

where

$$\bar{\bar{\bar{\theta}}}_i = C\left(\lambda_n, \xi_p, \eta_q, a, w, b, \theta_i\right) = \int_0^a\int_0^w\int_0^b \theta_i(\lambda_n \cos\lambda_n x + \gamma \sin\lambda_n x) \times (\xi_p \cos\xi_p y + \gamma \sin\xi_p y)\left(\eta_q \cos\eta_q z + \gamma \sin\eta_q z\right)dxdydz \tag{26}$$

Our next goal is to apply appropriate inversion techniques to obtain an analytical expression for temperature. First, the inverse Fourier transform in z direction, $\bar{\bar{\bar{\theta}}}(\lambda_n, \xi_p, z, t) = \sum_{q=1}^{\infty} K(\eta_q, z)\bar{\bar{\bar{\theta}}}(\lambda_n, \xi_p, \eta_q, t)$ is used to obtain transformed temperature as

$$\bar{\bar{\bar{\theta}}}(\lambda_n, \xi_p, z, t) = \sum_{q=1}^{\infty} \frac{\sqrt{2}\left(\eta_q \cos\eta_q z + \gamma \sin\eta_q z\right)}{\sqrt{b\left(\eta_q^2 + \gamma^2\right) + 2\gamma}}\bar{\bar{\bar{\theta}}}\left(\lambda_n, \xi_p, \eta_q, t\right) \tag{27}$$

Next the inverse Fourier transform for y direction, $\bar{\theta}(\lambda_n, y, z, t) = \sum_{p=1}^{\infty}\kappa(\xi_p, y)\bar{\bar{\bar{\theta}}}(\lambda_n, \xi_p, z, t)$ is applied to find second transformed temperature as

$$\bar{\theta}(\lambda_n, y, z, t) = \sum_{p=1}^{\infty}\sum_{q=1}^{\infty}\sqrt{4} \times \frac{(\xi_p \cos\xi_p y + \gamma \sin\xi_p y)\left(\eta_q \cos\eta_q z + \gamma \sin\eta_q z\right)}{\sqrt{\left(w\left(\xi_p^2 + \gamma^2\right) + 2\gamma\right)\quad\left(b\left(\eta_q^2 + \gamma^2\right) + 2\gamma\right)}} \times \bar{\bar{\bar{\theta}}}\left(\lambda_n, \xi_p, \eta_q, t\right) \tag{28}$$

Finally, the inverse Fourier transform for x direction, $\theta(x, y, z, t) = \sum_{n=1}^{\infty}\kappa(\lambda_n, x)\bar{\theta}(\lambda_n, y, z, t)$ is applied to find an analytic expression of temperature as

$$\theta(x, y, z, t) = \sum_{n=1}^{\infty}\sum_{p=1}^{\infty}\sum_{q=1}^{\infty} A\left(\lambda_n, \xi_p, \eta_q, x, y, z\right)\bar{\bar{\bar{\theta}}}\left(\lambda_n, \xi_p, \eta_q, t\right) \tag{29}$$

where $A(\lambda_n, \xi_p, \eta_q, x, y, z) = \sqrt{8}\frac{(\lambda_n \cos\lambda_n x + \gamma \sin\lambda_n x)(\xi_p \cos\xi_p y + \gamma \sin\xi_p y)(\eta_q \cos\eta_q z + \gamma \sin\eta_q z)}{\sqrt{(a(\lambda_n^2+\gamma^2)+2\gamma)(w(\xi_p^2+\gamma^2)+2\gamma)(b(\eta_q^2+\gamma^2)+2\gamma)}}$

Note that the above expression is only valid for a short period (τ) of electromagnetic heating. To obtain temperature distribution at any instant of time (t_f), we need to solve the Eq. (16) for N times, where $N = t_f/\tau$. For each time step, the initial condition for the Eq. (16) is the solution of previous time step starting with time, $t = 0$ and boundary conditions at any time are given by Eqs. (17b)–(17g). Thus, the close form analytical expression at t_f becomes

$$\theta(x, y, z, t_f) = T(x, y, z, t_f) - T_\infty = \sum_{n=1}^{\infty}\sum_{p=1}^{\infty}\sum_{q=1}^{\infty} A\left(\lambda_n, \xi_p, \eta_q, x, y, z\right) \times \left[\frac{\Phi(x, y, z, t_f - \tau)}{\alpha\left(\lambda_n^2 + \xi_p^2 + \eta_q^2\right)}\left(1 - e^{-\alpha\left(\lambda_n^2+\xi_p^2+\eta_q^2\right)\tau}\right)\right] + \sum_{n=1}^{\infty}\sum_{p=1}^{\infty}\sum_{q=1}^{\infty} A\left(\lambda_n, \xi_p, \eta_q, x, y, z\right) \times C\left(\lambda_n, \xi_p, \eta_q, a, w, b, \theta(x, y, z, t_f - \tau)\right)e^{-\alpha\left(\lambda_n^2+\xi_p^2+\eta_q^2\right)\tau} \tag{30}$$

4. Results and discussion

In this study close-form analytic expressions of electric field and temperature are obtained for electromagnetic heating of a 3D rectangular shaped object. Electromagnetic wave frequency ranges from radio frequency (27 MHz) to household microwave frequency (2450 MHz) is considered here. It is noteworthy to mention that the dielectric properties are a strong function of the working frequency as shown in Table 1. The other material properties are assumed to be constant for the simplicity in calculation and presented in Table 2. Although the analytic results presented in this study are valid for any 3D rectangular shaped object, for illustration purpose, we have considered temperature distribution in a salmon fillet (7 × 4 × 1.5 cm). We have specifically addressed the effect of temperature dependent dielectric properties in evaluating the source term from the electric field distribution and its consequence in the final temperature distribution. Although dielectric properties changes with temperature, they can be considered as temperature independent for short period of processing time as the temperature change is very low (<1 K) if the processing time is less than 1 s [19,22]. Hence our strategy is to calculate the temperature distribution for a short period of time (τ) by assuming constant property and update the source term in the energy equation (Eq. (16)) for the next time step using the latest temperature information. To estimate the temperature dependent source term, we derived empirical relations between dielectric properties of

Table 1
Temperature dependent dielectric properties for salmon fillets [22].

Frequency (MHz)	Dielectric constant, κ'	Dielectric loss, κ''
27	$\kappa' = -4e^{-04}T^2 + 0.6064T + 80.87$	$\kappa'' = 0.0429T^2 + 4.8592T + 365.74$
40	$\kappa' = 4e^{-05}T^2 + 0.3575T + 77.03$	$\kappa'' = 0.0284T^2 + 3.4078T + 248.51$
433	$\kappa' = 7e^{-04}T^2 - 0.1302T + 63.37$	$\kappa'' = 0.0027T^2 + 0.3865T + 29.49$
915	$\kappa' = 5e^{-04}T^2 - 0.1393T + 59.91$	$\kappa'' = 0.0015T^2 + 0.1498T + 19.47$
2450	$\kappa' = -0.0045T^2 + 0.4793T + 42.03$	$\kappa'' = -0.0012T^2 + 0.2616T + 12.45$

Table 2
Thermal properties and input parameters for analytic calculations.

Parameters	Values
Heat transfer coefficient, h (W/m^2)	1.5, 10, 25, 50
Specific heat capacity, c_p (J/kg K)	3589.40
Thermal conductivity, k (W/m K)	0.4711
Density, ρ (kg/m^3)	1047.89
Initial temperature, T_i (°C)	20
Surrounding temperature, T_∞ (°C)	20
Thickness of salmon fillet, b (cm)	1.5
Incidence electromagnetic energy flux, I (W/cm^2)	3.00
Length of salmon fillet, a (cm)	7
Width of salmon fillet, w (cm)	4

salmon fillet and temperature (Table 1) from experimental data [22] using statistical regression. The algorithm used to calculate the temperature distribution is shown in Fig. 2.

All temperature results presented in this study are for the two-sided heating cases, though analytical expressions for electric field and source term distribution are presented for both one-sided and two-sided electromagnetic heating. One can easily find the temperature distribution for one-sided heating using the expression shown in Eq. (13b). In this study, the incidence microwave energy flux ($I = 0.5c\varepsilon_0 E^2$) was kept constant at 3 W/cm^2; this value corresponds to a 1.2 kW household microwave. For the rest of the paper, the microwave frequency and convective heat transfer coefficient are varied from case to case to elucidate the comprehensive effect on temperature distribution during electromagnetic heating.

To validate the algorithm proposed above (Fig. 2), we have solved the energy equation (Eq. (14)) numerically for convective boundary conditions (Eqs. (15b)–(15g)) with temperature dependent source term. The finite element (numerical) solution is obtained by COMSOL 3.2 using general PDE mode where we solved the coupled Maxwell's equation (Eq. (5)) and unsteady energy equation (Eq. (14)) with temperature dependent dielectric properties as shown in Table 1. Fig. 3 shows comparison between numerical and analytic results for 75 s of electromagnetic heating with temperature dependent source term. The temperature distributions along the propagation (z) direction are extracted from the 3D solution at the center point of the fillet. Four different electromagnetic frequencies, radio frequency (40 MHz) and microwave frequencies (433, 915 and 2450 MHz) which are allocated by the US Federal Communications Commission (FCC) for industrial heating and microwave oven systems, are used to illustrate the temperature distribution within the system.

The temperature results between the numerical method and the proposed analytical technique have matched perfectly validating the method presented here. Fig. 3 also presents the temperature distributions for constant dielectric properties. It is evident that analytic results with constant dielectric properties over-predict the temperature distribution for the radio frequency ($f = 40$ MHz) as shown in Fig. 3(a). This is because of the fact that the penetration depth, a length scale at which the incident energy reduces to its 1/e th value, decreases with temperature for the

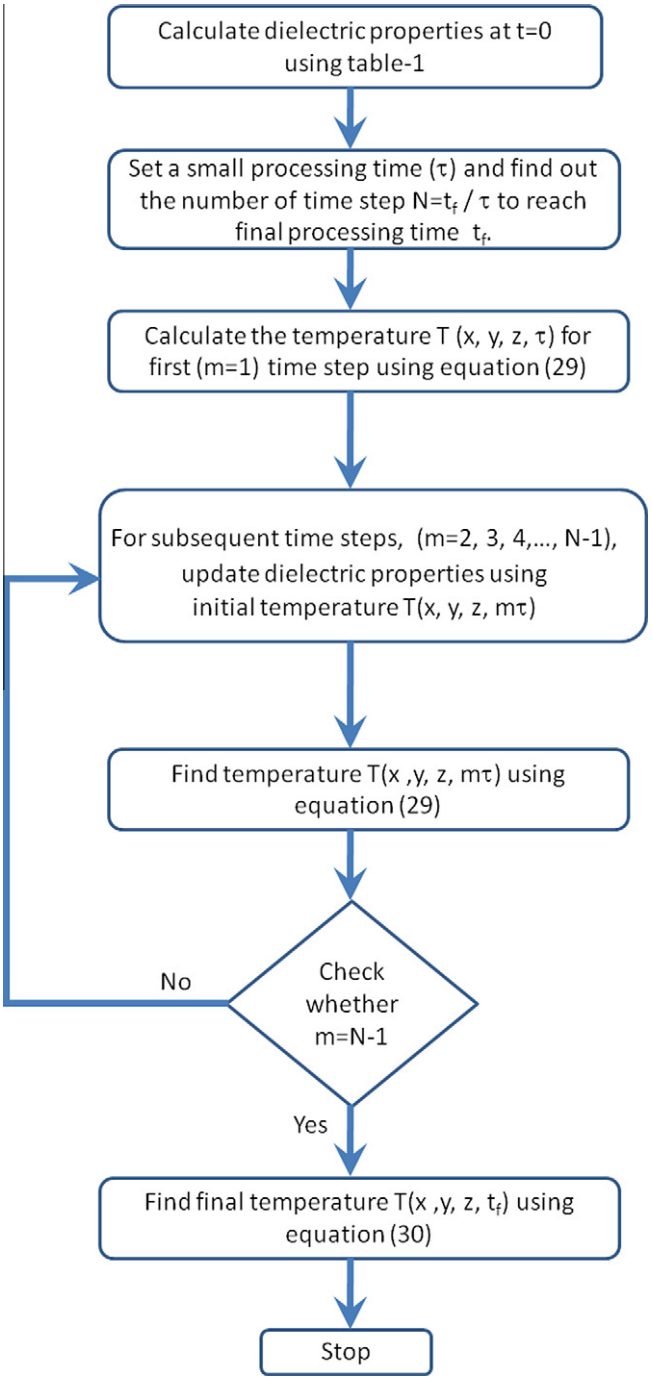

Fig. 2. Algorithm used to calculate temperature distribution within a sample using temperature dependent dielectric properties.

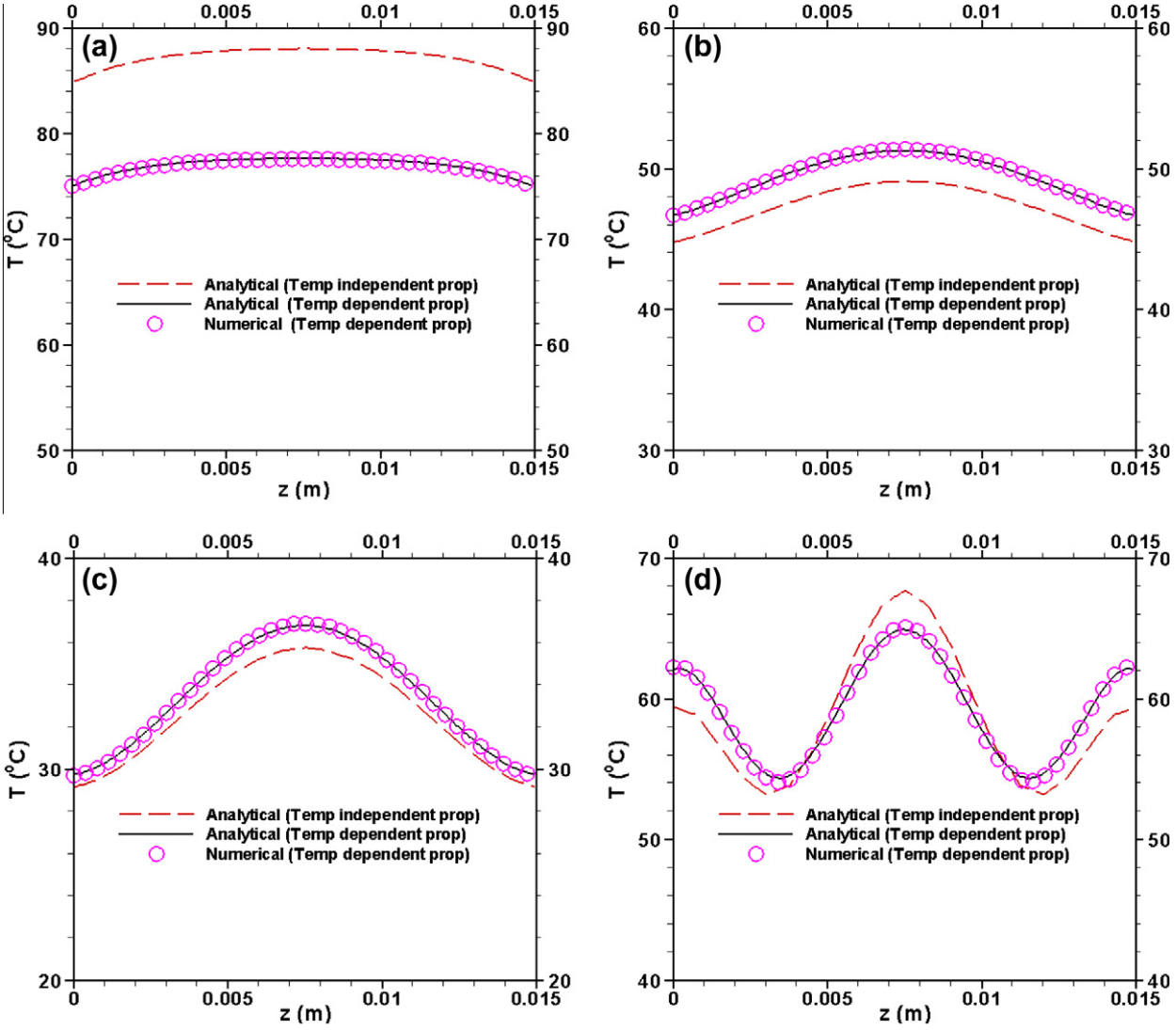

Fig. 3. The comparison between numerical and analytic results for temperature distribution with and without temperature dependent dielectric properties for various electromagnetic frequencies. Electromagnetic frequencies are (a) $f = 40$ MHz, (b) $f = 433$ MHz, (c) $f = 915$ MHz, and (d) $f = 2450$ MHz. The convective heat transfer coefficient is 10 W/m^2 K.

radio frequency heating which retards the transmission of electromagnetic waves. On the other hand, for low range of microwave frequencies ($f = 433$ MHz and 915 MHz) the constant dielectric properties under-predict the temperature within the body. This under prediction can be explained from the relationship among dielectric properties and temperature. Dielectric properties are expressed by two parameters: dielectric constant (κ') and dielectric loss (κ''). The dielectric loss is a measure of heat dissipation in the body and the dielectric constant quantifies the energy storing ability. For lower range of microwave frequency, the dielectric constant decreases slightly with temperature while the dielectric loss increases with temperature. That means, for variable dielectric properties an object will be able to dissipate more heat with time and the temperature will be higher than the constant dielectric properties case. However, the temperature difference between constant and variable (temperature dependent) dielectric cases are much less for the microwave heating than that of the radio frequency heating. Interestingly, at the domestic microwave oven frequency ($f = 2450$ MHz), the dielectric properties are not a strong function of temperature. Hence, both constant and variable dielectric properties predict almost similar temperature, and the minor discrepancy is due to the small change in properties. In other words, the constant dielectric property based temperature prediction is acceptable for the frequency used in the household microwave oven.

Next we present the three dimensional temperature profiles in a salmon fillet with temperature dependent dielectric properties for microwave (Fig. 4(a)) and radio frequency heating (Fig. 4(b)). The absorbed electromagnetic power is used as a volumetric heat generation term in the energy equation, and hence distribution of generation term mainly dictates the temperature distribution in the fillet. For radio frequency heating the generation term is almost uniform in the propagation direction due to much longer penetration depth. On the other hand, for microwave heating, the volumetric heat absorption depends on the electromagnetic frequency and thickness of the object in addition to the dielectric properties [21]. For identical heating power and time, the radio frequency heating is able to generate higher temperature increase than microwave heating.

We also extracted the temperature distribution at different x–y planes from the 3D contour plot, and shown in Figs. 4(c) and (d) for microwave and radio frequency heating. Due to the sym-

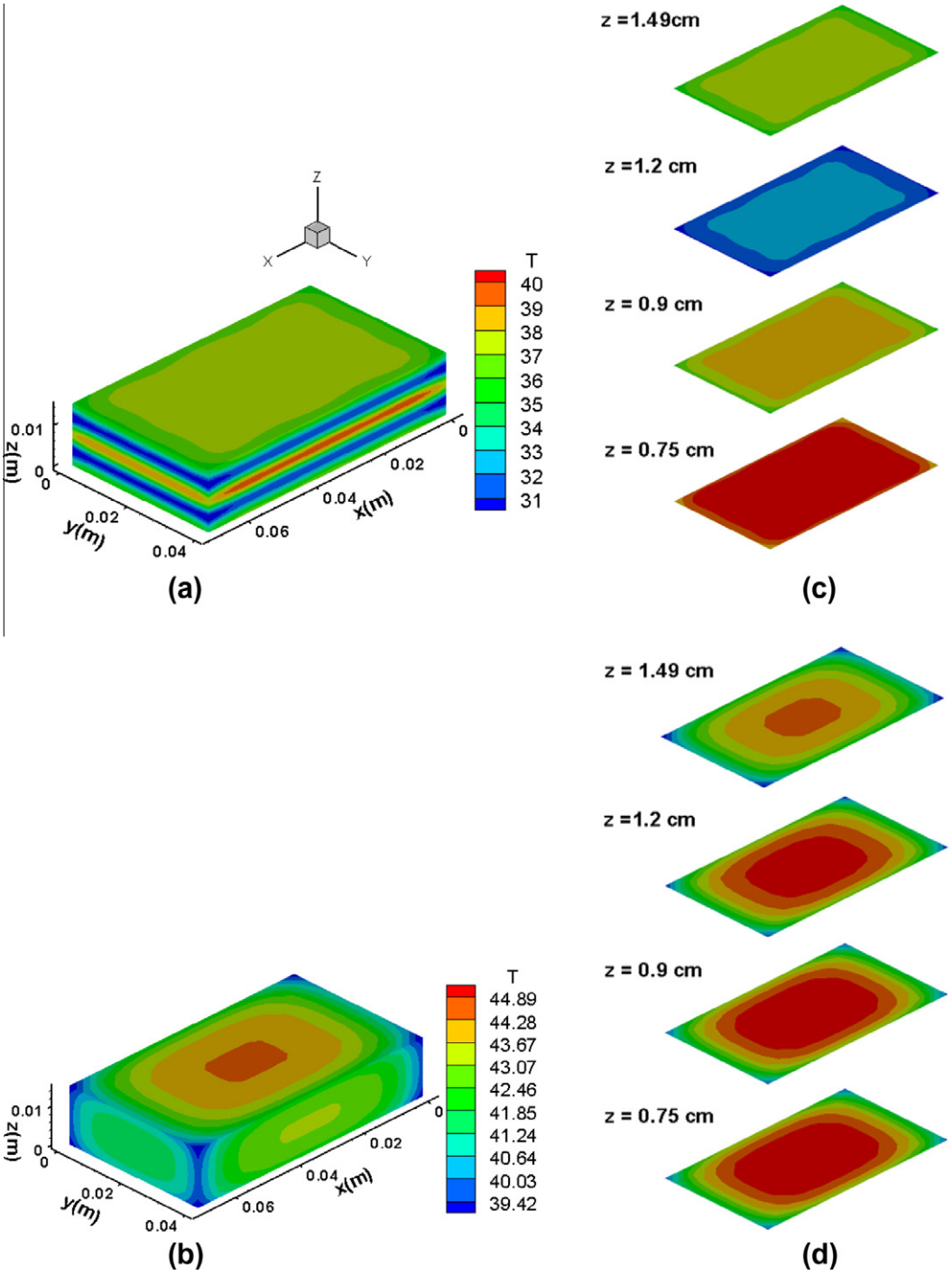

Fig. 4. Temperature distribution for 30 s electromagnetic heating of 7 × 4 × 1.5 cm salmon fillet. (a & b) three dimensional contour for f = 2450 MHz and f = 40 MHz. (c & d) Illustration of temperature distribution at four different planes for microwave (f = 2450 MHz) and radio frequency (f = 40 MHz) heating. The convective heat transfer coefficient is 10 W/m^2 K.

metry in the heating conditions, the temperature profiles are presented for four selected planes at the upper half of the fillet. For radio frequency heating (Fig. 4(d)), the temperature at a particular point remains almost uniform at different sections (z-location) of fillet, but significant changes in temperature are evident for the microwave heating (Fig. 4(c)). The variations in temperature do exist in the x–y plane for both radio frequency and microwave heating due to convection heat transfer from the boundaries.

The effect of electromagnetic wave frequency on temperature rise is shown in Fig. 5 for 75 s processing of 1.5 cm thick salmon fillet. In this case two-dimensional temperature contours are presented along the x–z plane at y = 2 cm for a convective heat transfer coefficient of 10 W/m^2 K. For this type of convective heat transfer from boundary, the temperature profile remains almost one dimensional except very close to the edge. Again the temperature distribution along the propagation direction is greatly influenced by the wave frequency. For lower frequency, the temperature distribution is more uniform, but heterogeneity in temperature is observed for the microwave heating with alternate hot and cold spots especially for the domestic microwave oven (f = 2450 MHz) heating.

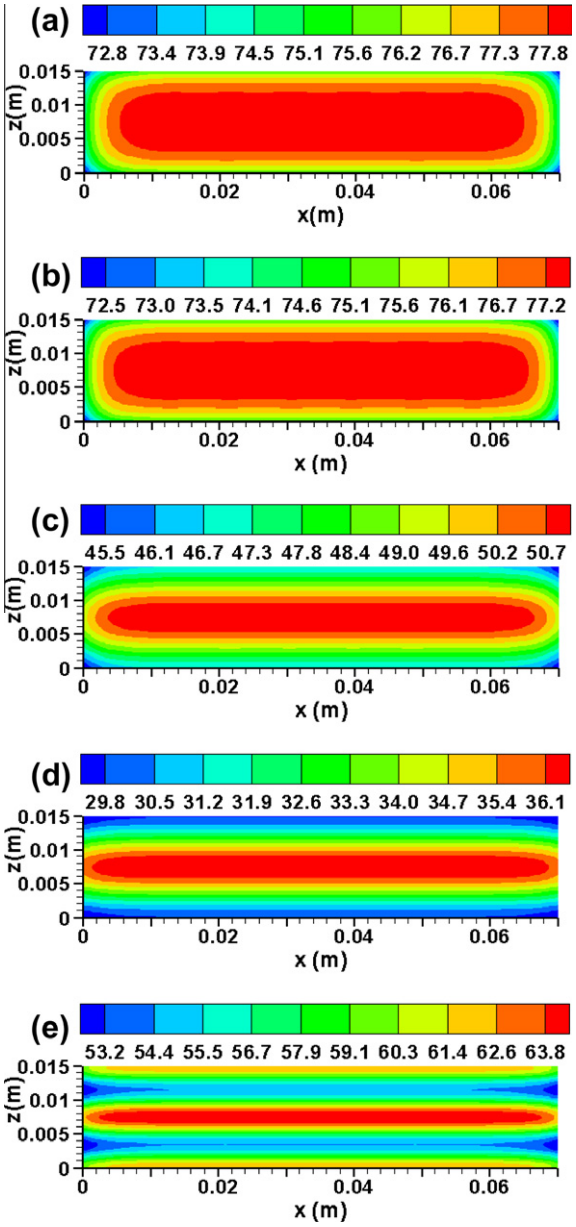

Fig. 5. Two dimensional temperature contours for 75 s electromagnetic heating of $7 \times 4 \times 1.5$ cm salmon fillet at y = 0.02 m plane. Electromagnetic frequencies are (a) $f = 27$ MHz, (b) $f = 40$ MHz, (c) $f = 433$ MHz, (d) $f = 915$ MHz, and (e) $f = 2450$ MHz.

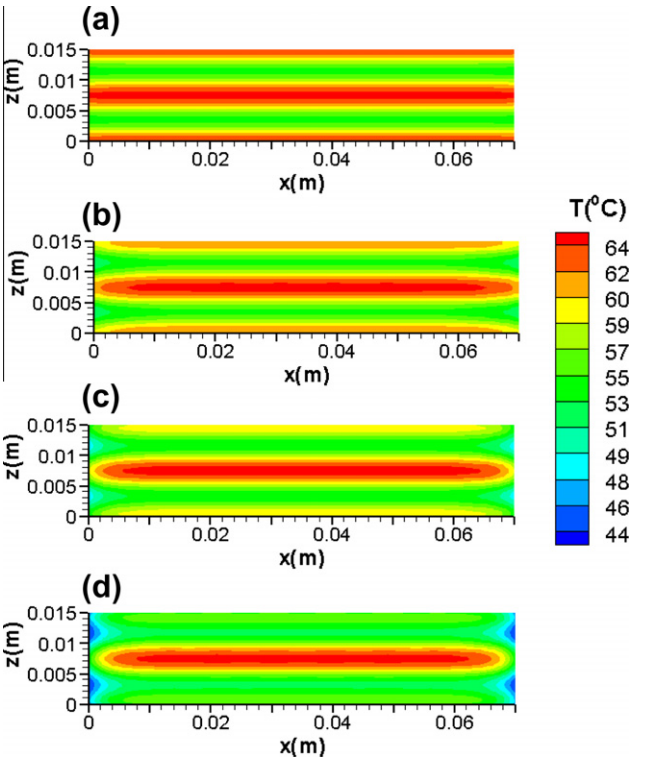

Fig. 6. Two dimensional (x–z) temperature contours for 75 s microwave heating of $7 \times 4 \times 1.5$ cm salmon fillet at $y = 0.02$ m and $f = 2450$ MHz. Heat transfer coefficients are (a) $h = 1.5$ W/m^2 K, (b) $h = 10$ W/m^2 K, (c) $h = 25$ W/m^2 K, and (d) $h = 50$ W/m^2 K.

Fig. 6 illustrates the effect of heat transfer coefficient on electromagnetic heating of a salmon fillet at the 2450 MHz frequency. Two dimensional temperature results are presented along the x–z plane for 75 s of microwave heating. The surfaces of the fillet are cooled by the convective heat transfer to the surrounding air space. For 1.5 cm thick sample, core heating as well as surface heating take place for 2450 MHz frequency if the convective heat transfer coefficient is small. With the increase in heat transfer coefficient, the surface heating gets reduced because of the higher heat transfer rate from the outer surfaces, but the core heating remains less affected. This is because of the fact that the salmon fillet has much lower thermal conductivity and hence, the heat diffusion rate is much slower than the generation rate. Thus by increasing the heat transfer coefficient, one can avoid surface heating, but not the core heating. Core heating can be avoided by pulsating the electromagnetic waves [27]. It is claimed in literature that a pulsating microwave might provide better temperature distribution because the pulsating time could make up the lag time between the generation and the thermal transport by conduction [27]. Other thermal properties such as specific heat of the material are also important in electromagnetic heating (not shown in figures). A material with lower specific heat requires less energy for unit change of temperature. For example, fats and oils heat up quickly in microwave due to their low specific heat capacity, although they have relatively low dielectric properties [10]. Therefore, the heat transfer coefficient along with the other thermal properties of foodstuff need to be integrated with the factors such as geometry, dielectric properties to predict the accurate temperature distribution.

The one dimensional temperature distributions along the z directions at the center of the fillet are shown in Fig. 7 for various electromagnetic frequencies and processing time. For the same incident energy flux and time, 40 MHz frequency provides higher temperature because at this frequency the salmon fillet possesses higher dielectric loss for which it can dissipates energy much faster rate than any other frequency. The power distribution results presented in Fig. 7 reveals that the volumetric heat generation decreases with time for the radio frequency processing, but increases moderately or slightly for the microwave heating. The decrease in power absorption for radio frequency ($f = 40$ MHz) is due to the lower penetration depth at higher temperature as described earlier. On the other hand, the slight increase in power absorption for $f = 433$ and 915 MHz is due to increase in the dielectric loss with temperature. Since the dielectric properties is a weak function of temperature for $f = 2450$ MHz, the power absorption remain unaltered with time.

Fig. 7 also shows that the temperature distribution becomes almost uniform for radio frequency heating, which is highly desirable from food safety point of view. On the other hand, the alternate hot and cold spots are noticed for higher frequency microwave especially for $f = 2450$ MHz. Similar nonuniform

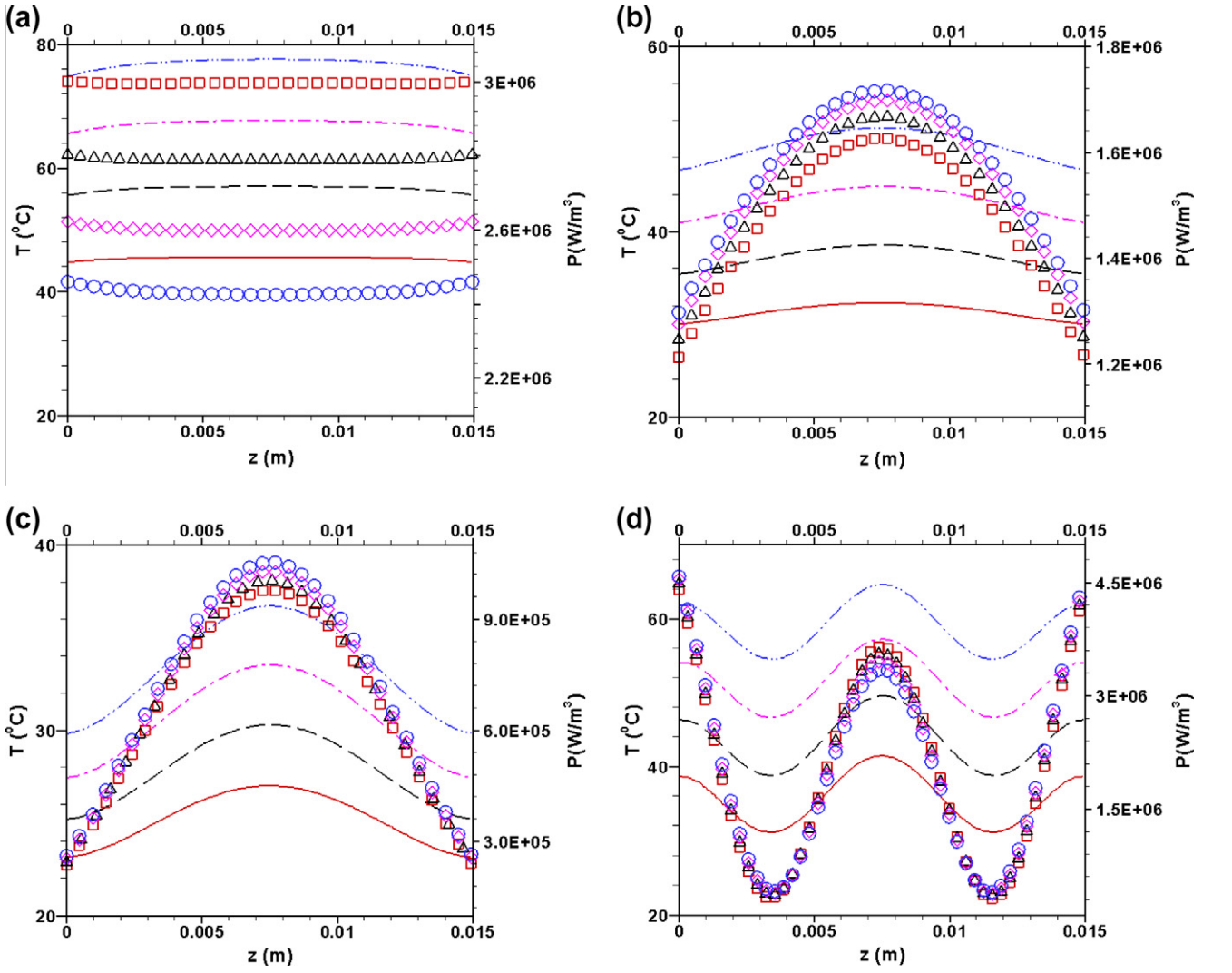

Fig. 7. The center line temperature distribution ($t = 30$ s; $t = 45$ s; $t = 60$ s and $t = 75$ s) along with electromagnetic power absorption ($t = 30$ s; $t = 45$ s; $t = 60$ s and $t = 75$ s) for various processing time within a $7 \times 4 \times 1.5$ cm salmon fillet for electromagnetic heating. The temperature results are extracted at $x = 3.5$ cm and $y = 2$ cm, and the convective heat transfer coefficient is 10 W/m^2 K. Electromagnetic frequencies are (a) $f = 40$ MHz, (b) $f = 433$ MHz, (c) $f = 915$ MHz, and (d) $f = 2450$ MHz.

temperature results have been presented in the past for microwave heating [20–21]. As a matter of fact, temperature distributions directly follow the power absorption trends. As seen from the microwave power absorption (Fig. 7(b)–(d)), the occurrence of resonance during microwave heating attributes to unusually large local heating rates and facilitates greater heterogeneity in temperature distribution. At 2450 MHz, the salmon fillet experiences two resonances which is the worst situation for temperature distribution [21]. The formation of peaks and dips can be explained from the wavelength of the electromagnetic wave. The wavelength within a sample is a function of the wave frequency, temperature, and dielectric properties. For a particular size of a salmon fillet, the wavelength generally decreases with the increase of temperature and frequency. As the wavelength decreases, more resonances (peak and dip) formed in the sample. Conversely, for the radio frequency heating, the wavelength is much larger than the sample thickness. Because of longer wavelength, radio frequency wave can penetrate deeper and can avoid surface heating and occurrence of alternate hot and cold spots within the object. Although wavelength changes slightly with temperature, it is not large enough to make any nonuniformity in the temperature distribution for the radio frequency heating (Fig. 7(a)).

It is interesting to note that the temperature increases monotonically without altering the temperature distribution for all frequencies (Fig. 7). An increased processing time allows more friction and alterations of dipoles/molecules in a given specimen and provides elevated temperature. The difference between maximum and minimum temperature also increases with time. The differences between maximum and minimum temperature at processing time of 75 s for 40, 433, 915 and 2450 MHz are 4.7, 5.2, 6.3 and 10.6 °C, respectively.

5. Summary and conclusions

An analytical expression with an adaptive algorithm for temperature distribution is presented for a rectangular block whose dielectric properties are temperature dependent during electromagnetic heating. The electromagnetic power absorption is obtained from Maxwell's equation, and is used as a non-linear generation term in a three dimensional, unsteady, heat equation. The non homogenous heat equation is solved using integral transform techniques. The temperature distribution within a salmon fillet shows that using proposed algorithm one can predict the

solution of non-linear energy equation from constant property analytical solution. We also presented a rigorous discussion on the effect of frequency, dielectric properties, and heat transfer coefficient on temperature distribution in electromagnetic heating. This study results in following conclusions.

(1) For constant value of dielectric properties, the analytical solution of temperature over-predict and under-predict for radio frequency and lower frequency range microwave heating, respectively.
(2) For frequency above 2000 MHz, both constant and variable (temperature dependent) properties provide identical temperature profile.
(3) In electromagnetic heating the temperature profile closely follow the power absorption distribution except very close to the surface where the influence of convective heat transfer is present.
(4) The volumetric power absorption decreases with temperature for the radio frequency heating, but its value increases or remain same for the microwave heating.
(5) The temperature distribution in salmon fillet reveals that electromagnetic heating with lower frequency waves provides better temperature distribution. In particular, the radio frequency heating gives almost uniform temperature distribution.
(6) With same incident energy flux, the radio frequency provides faster heating compared to microwave heating.
(7) In addition to other thermo-physical properties, the heat transfer coefficient of the surroundings has significant impact on temperature distribution.

References

[1] S. Curet, O. Rouand, L. Boillereaux, Microwave tempering and heating in a single-mode cavity: numerical and experimental investigations, Chem. Eng. Process. 47 (2008) 1656–1665.
[2] K.F. Lei, S. Ahsan, N. Budraa, W.J. Li, J.D. Mai, Microwave bonding of polymer-based substrate for potential encapsulated micro/naofluidic device fabrication, Sensors Actuat. A 114 (2004) 340–346.
[3] M. Rahbar, S. Chhina, D. Sameoto, M. Parameswarn, Microwave-induced, thermally assisted solvent bonding for low-cost PMMA microfluidic devices, J. Micromech. Microeng. 20 (2010) 15–26.
[4] D. Issadore, K.J. Humphry, K.A. Brown, L. Sandberg, D.A. Weitz, R.M. Westervelt, Microwave dielectric heating of drops in microfluidic devices, Lab Chip 9 (2009) 1701–1706.
[5] J.J. Shah, S.G. Sundaresan, J. Geist, D.R. Reyes, J.C. Booth, M.V. Rao, M. Gaitan, Microwave dielectric heating of fluids in an integrated microfluidic device, J. Micromech. Microeng. 17 (2007) 2224–2230.
[6] C.O. Kappe, D. Dallinger, The impact of microwave synthesis in drug discovery, Nature 5 (2006) 51–64.
[7] K.G. Ayappa, H.T. Davis, G. Crapiste, E.A. Davis, J. Gordon, Microwave heating an evaluation of power formulations, Chem. Eng. Sci. 46 (4) (1991) 1005–1016.
[8] E.O. Goksoy, C. James, S.J. James, Non-uniformity of surface temperatures after microwave heating of poultry meat, J. Microw. Power Electromagn. Energ. 34 (3) (1999) 149–160.
[9] V. Romano, F. Marra, A numerical analysis of radio frequency heating of regular shaped foodstuff, J. Food Eng. 84 (2008) 449–457.
[10] J.Y. Jeong, E.S. Lee, J.H. Choi, J.Y. Lee, J.M. Kim, S.G. Min, Y.C. Chae, C.J. Kim, Variability in temperature distribution and cooking properties of ground pork patties containing different fat level and with/without salt cooked by microwave energy, Meat Sci. 75 (2007) 415–422.
[11] F. Marra, J. Lyng, V. Romano, B. McKenna, Radio-frequency heating of foodstuff: solution and validation of a mathematical model, J. Food Eng. 79 (2007) 998–1006.
[12] W. Guo, S. Wang, G. Tiwari, J.A. Johnson, J. Tang, Temperature and moisture dependent dielectric properties of legume flour associated with dielectric heating, Food Sci. Technol. 43 (2010) 193–201.
[13] P. Piyasena, C. Dussault, T. Koutchma, H.S. Ramaswamy, G.B. Awuah, Radio frequency heating of foods: principles, applications and related properties – a review, Crit. Rev. Food Sci. Nutr. 43 (6) (2003) 587–606.
[14] C.J. Budd, A.D.C. Hill, A comparison of models and methods for simulating the microwave heating of moist foodstuffs, Int. J. Heat Mass Transfer 54 (2011) 807–817.
[15] H. Ni, A.K. Datta, K.E. Torrance, Moisture transport in intensive microwave heating of biomaterials: a multiphase porous media model, Int. J. Heat Mass Transfer 42 (1999) 1501–1512.
[16] N. Sakai, C. Wang, An analysis of temperature distribution in microwave heating of foods with non-uniform dielectric properties, J. Chem. Eng. Jpn. 37 (7) (2004) 858–862.
[17] W. Cha-um, P. Ratttanadecho, W. Pakdee, Experimental and numerical analysis of microwave heating of water and oil using a rectangular wave guide: influence of sample sizes, positions, and microwave power, Food Bioprocess. Technol. 23 (2009) 544–558.
[18] P. Rattanadecho, Theoretical and experimental investigation of microwave thawing of frozen layer using a microwave oven (effects of layered configurations and layer thickness), Int. J. Heat Mass Transfer 47 (5) (2004) 937–945.
[19] K.G. Ayappa, H.T. Davis, E.A. Davis, J. Gordon, Analysis of microwave heating of materials with temperature dependent properties, AIChE J. 37 (3) (1991) 313–322.
[20] G.J. Fleischman, Predicting temperature range in food slabs undergoing short-term/high-power microwave heating, J. Food Eng. 40 (1999) 81–88.
[21] M.R. Hossan, D.Y. Byun, P. Dutta, Analysis of microwave heating for cylindrical shaped objects, Int. J. Heat Mass Transfer 53 (2010) 5129–5138.
[22] Y. Wang, J. Tang, B. Rasco, F. Kong, S. Wang, Dielectric properties of salmon fillets as a function of temperature and composition, J. Food Eng. 87 (2008) 236–246.
[23] S.O. Nelson, P.G. Bartley Jr., Measuring frequency and temperature dependent properties of food material, Trans. ASAE 43 (6) (2000) 1733–1736.
[24] B. Zhou, S. Avramidis, On the loss factor of wood during radio frequency heating, Wood Sci. Technol. 33 (1999) 299–310.
[25] G. Roussy, J.A. Pearce, Foundations and Industrial Applications of Microwaves and Radio Frequency Fields-Physical and Chemical Processes, John Wiley and Sons Ltd., West Sussex, England, 1995. pp. 7–25.
[26] S. Kakac, Y. Yener, Heat Conduction, second ed., Hemisphere, New York, 1985. pp. 244–270.
[27] S. Gunasekaran, Pulsed microwave-vacuum drying of food materials, Dry. Technol. 17 (3) (1999) 395–412.